Random time step probabilistic methods for uncertainty quantification in chaotic and geometric numerical integration

Assyr Abdulle* and Giacomo Garegnani†

Abstract. A novel probabilistic numerical method for quantifying the uncertainty induced by the time integration of ordinary differential equations (ODEs) is introduced. Departing from the classical strategy to randomize ODE solvers by adding a random forcing term, we show that a probability measure over the numerical solution of ODEs can be obtained by introducing suitable random time-steps in a classical time integrator. This intrinsic randomization allows for the conservation of geometric properties of the underlying deterministic integrator such as mass conservation, symplecticity or conservation of first integrals. Weak and mean-square convergence analysis are derived. We also analyse the convergence of the Monte Carlo estimator for the proposed random time step method and show that the measure obtained with repeated sampling converges in mean-square sense independently of the number of samples. Numerical examples including chaotic Hamiltonian systems, chemical reactions and Bayesian inferential problems illustrate the accuracy, robustness and versatility of our probabilistic numerical method.

AMS subject classifications. 65C30, 65F15, 65L09

Key words. Probabilistic methods for ODEs, random time steps, uncertainty quantification, chaotic systems, geometric integration, inverse problems.

1. Introduction.

A variety of methods for integrating ordinary differential equations (ODEs) has been studied in the last decades, [8, 9, 7], with an emphasis on building accurate and stable deterministic approximations of the exact solution. In general, these methods are based on a time discretisation on which the solution of the ODE is approximated via an iterative deterministic algorithm. Given a time step h, which indicates the refinement of the discretisation, all these methods provide a punctual value for the approximation of the solution. While it is guaranteed that in the asymptotic limit of $h \to 0$ the numerical approximation will coincide with the exact solution, it is not possible for a fixed value of $h > 0$ to quantify exactly the error that is committed in numerical integration. The information that is provided a priori on the quality of the solution is that the error will be proportional to a positive power q of the time step, i.e., the order of convergence. Nonetheless, in order to obtain accurate solutions, it could be required to set h small and the computational power deriving from this choice could be unbearable in modern applications.

In recent years, probabilistic numerical methods for differential equations have been proposed [6, 4, 11] in order to quantify the uncertainty introduced by the time discretization in a statistical manner. In general, these methods proceed iteratively to establish a probability measure over the numerical solution, thus providing a richer information than a single punctual value. In particular, probabilistic solvers offer a quantitative characterization of late time errors by tuning the noise introduced by the method according to the accuracy of the solver. In this way, it is possible to obtain a reliable approach for capturing the sensitivity

*Mathematics Section, École Polytechnique Fédérale de Lausanne (assyr.abdulle@epfl.ch)
†Mathematics Section, École Polytechnique Fédérale de Lausanne (giacomo.garegnani@epfl.ch)

of the solution to numerical error, while transferring the convergence properties of classical deterministic integrators to the introduced probability measure in a consistent manner.

In the following, we will first show three examples motivating the probabilistic approach, and then present the main contributions of this work.

1.1. Motivating examples. Probabilistic integrators for ODEs do not provide with more accurate solutions than classical deterministic methods. Nevertheless, their usefulness is evident in a variety of different problems, among which we identified the integration of chaotic dynamical systems, the proposal of reliable a posteriori error estimators and the solution of Bayesian inverse problems, which are briefly presented here.

Chaotic differential equations. Let us consider the Lorenz system [14], which is defined by the following ODE

$$\begin{aligned} x' &= \sigma(y-x), & x(0) &= -10, \\ y' &= x(\rho - z) - y, & y(0) &= -1, \\ z' &= xy - \beta z, & z(0) &= 40. \end{aligned} \tag{1.1}$$

It is well-known that for $\rho = 28$, $\sigma = 10$, $\beta = 8/3$, this equation has a chaotic behaviour, i.e., a small perturbation forces the trajectories to deviate from the true solution. Integrating numerically (1.1) the error which is introduced at each time step is indeed a perturbation, thus any numerical solution cannot be considered reliable. In order to explore the state space of this chaotic dynamical system, we introduce a random perturbation on the initial condition, implemented as a scalar Gaussian random variable $\varepsilon \sim \mathcal{N}(0, \sigma^2)$ and artificially added to the first component $x(t)$ at time $t = 0$. In Figure 1 we show $M = 20$ numerical trajectories given by a second-order Runge-Kutta method for three different scales σ of the noise. It is possible to remark that in all the three cases, the numerical solutions almost coincide up to some time $\bar{t}$, thus diverging and showing the chaotic nature of the Lorenz system. It could be argued that up to time $\bar{t}$, the numerical solution offers a reliable approximation of the true solution as the dynamics have not yet switched to the chaotic regime. Nevertheless, it is unclear how to choose σ so that the amount of noise that is introduced is balanced with the numerical error. Probabilistic methods for differential equations as the one presented in this work and the one introduced by Conrad et al. [6] provide with a rigorous analysis that suggests how to introduce a source of artificial noise in a consistent manner.

A reliable a posteriori error estimator for ODEs?. Building an accurate and reliable a posteriori error estimator for the numerical solution of ODEs is still an open problem in numerical analysis. Nonetheless, there exist many state of the art heuristic procedures to estimate the error and thus choose optimal time steps for integration. The common ground of these procedures is the choice of a tolerance value, that we denote by η, that should be respected in terms of the distance of the numerical solution from the true solution at final time. Apart from asymptotic analysis as the ones in [10, 12], where the limit for $\eta \to 0$ is analysed, there is no theoretical guarantee that the error estimators are indeed a bound for the true error.

A classical approach is given by the so-called embedded methods, where numerical errors are estimated employing locally an higher order integrator. Let us consider again the Lorenz

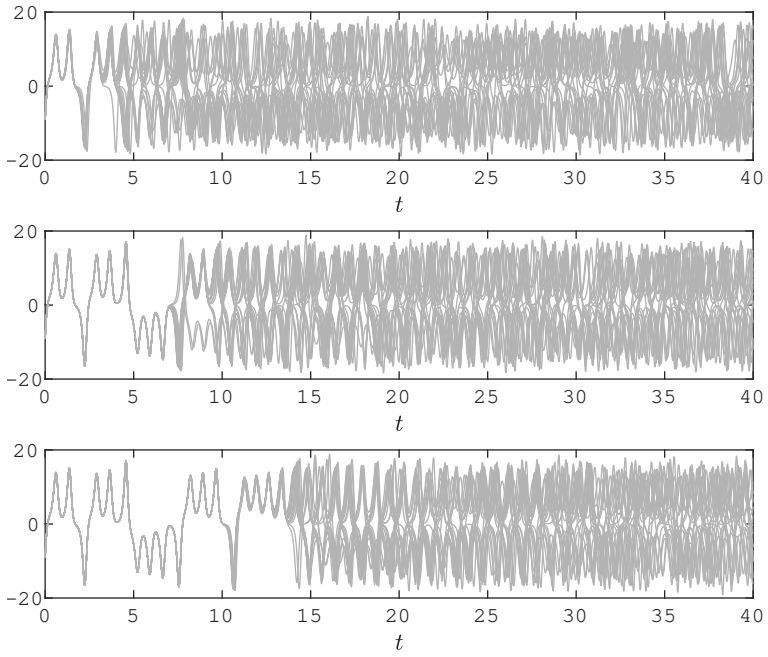

Figure 1: First component $x(t)$ of the solution of (1.1) with decreasing Gaussian perturbations on the initial condition from top to bottom.

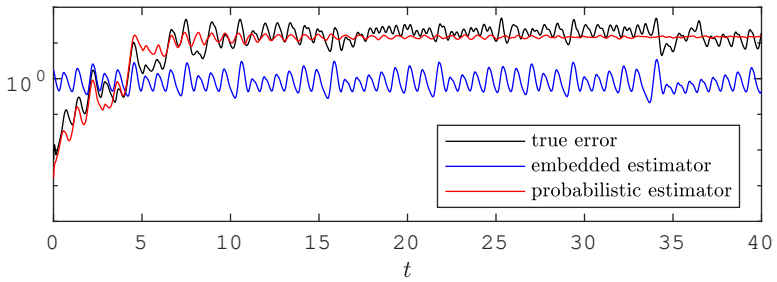

Figure 2: True error for the Lorenz system (black line), together with the error estimators given by the embedded couple explicit Euler – Heun (blue line) and by the standard deviation $\sigma(Y_n)$ of a probabilistic solution (red line).

system (1.1) with the same initial condition and values of the parameters as above. We integrate it employing the embedded couple of explicit Euler and Heun methods, which are respectively a first and a second order method, to estimate the error at each time. In Figure 2 we show that this traditional error estimator is not a reliable indicator of the true error.

A family of probabilistic solutions could give a consistent information on the numerical error. Let us denote by Y_n the solution given by the explicit Euler method perturbed in a probabilistic manner and by $\sigma(Y_n) = (\mathrm{tr}(\mathrm{Var}\, Y_n))^{1/2}$ its standard deviation, which could mimic the numerical error. We show in Figure 2 that σ_n indeed follows qualitatively the true error in a more accurate way than the deterministic approach of embedded methods.

Bayesian inverse problems. The most employed example to justify the usefulness of probabilistic methods for differential equations is given by Bayesian inverse problems. The impact of a probabilistic component in the numerical approximation of inverse problems involving ODEs has already been presented in several works (e.g., [6, 4, 5]). In particular, the common underlying idea of these works is that if a deterministic integrator with a fixed finite time step is employed to approximate the solution of the ODE appearing in an inferential problem, the numerical error introduced by deterministic solvers can lead to inappropriate and non-predictive posterior concentrations. In the limit of an infinitely refined time discretisation the posterior distributions obtained with a classical numerical method will indeed tend to the true distribution, but for a fixed time step (i.e., a fixed computational budget) results could be misleading. These inappropriate solutions to inverse problems can be easily corrected employing a probabilistic integrator to solve the ODE, thus obtaining posterior distributions that reflect the uncertainty given by the numerical solver.

1.2. Contributions. The method we analyse in this paper is inspired from the work of Conrad et al. [6], where one of the first probabilistic methods for ODEs is presented. The method they propose consists in constructing a probability measure employing a slight modification of one-step deterministic methods such as, for example, integrators belonging to the Runge-Kutta class. In particular, they propose to perturb the deterministic numerical solution with an additive source of noise at each time step. Scaling opportunely the random term, they manage to obtain a probabilistic solution without altering the convergence of the underlying deterministic scheme.

An additive noise contribution could nonetheless produce disruptive effects on favourable geometric features of deterministic schemes. A direct example of this non-robust behaviour is given by ODEs for which the solution is supposed to stay positive and small. In this case, the addition of a random contribution could force the solution in the negative plane, hence the numerical solution could be physically meaningless. Chemical reactions with small population size for one species at some time of the evolution is a typical physical example of such a situation. An additive random term could force the solution on the negative plane with a non-zero probability, which can become significantly big in case the magnitude of one component is small.

Motivated by this undesirable property, we present in this work a new probabilistic method for ODEs based on a random selection of the time steps, hence turning the stochastic component of the numerical solution from additive to intrinsic to the scheme itself. For this new robust probabilistic integrator, we are able to prove strong and weak convergence towards the exact solution of the underlying ODE. Precisely, setting the variance of the random time steps to be proportional to some power of a deterministic time step allows to retrieve the rates of the underlying Runge-Kutta integrator.

It has been pointed out by Kersting and Hennig [11] that probabilistic methods based on sampling should be equipped with a criterion to choose the number of samples, so that computational effort is not wasted or, conversely, the sample size is not insufficient to describe the dynamics in a probabilistic fashion. In order to address this issue, in this work we show that Monte Carlo estimators drawn from our probabilistic solver converge with respect to the time step in the mean square sense independently of the sample size. We are able to prove a

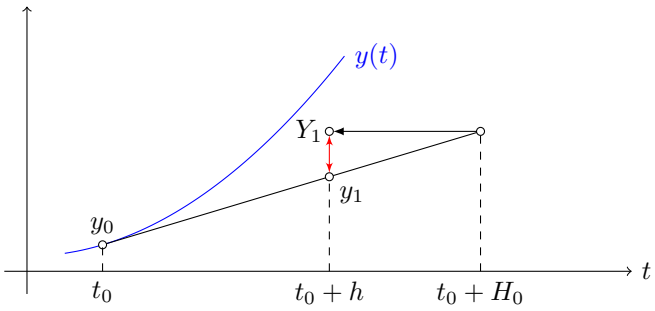

Figure 3: Graphical representation of one step of the RTS-RK method with $\Psi_h(y) = y + hf(y)$. The red arrow is the stochastic contribution due to random time-stepping.

similar property for the scheme proposed in [6].

A large variety of dynamical systems is characterised by geometrical properties of their flow map [7]. Most notably, Hamiltonian systems, which are employed for modelling a variety of physical phenomena, are endowed with the property of symplecticity. It is possible to obtain good approximations of the solutions of Hamiltonian systems via mimicking numerically the geometric properties of the exact flow, i.e., employing symplectic integrators. In particular, for symplectic integrators the energy function conserved by the exact flow is approximately conserved by numerical trajectories over long time spans, which in turn guarantees high-quality solutions at the price of a rather low computational effort.

While geometric properties of Runge-Kutta schemes have been analysed extensively in the deterministic case, they have not been considered yet for probabilistic numerical methods. The method we present in this work, being only an intrinsic modification of a Runge-Kutta integrator, is endowed with the geometric properties of its deterministic counterpart. In particular, we first show that our probabilistic scheme inherits the property of exact conservation of first integrals of motion. Then, we show that in Hamiltonian systems the good approximation of the energy function given by symplectic schemes is not spoilt by our randomisation procedure over polynomially long time spans.

1.3. Outline. The paper is organised as follows. In section 2 we introduce the setting for probabilistic numerics and present our novel numerical scheme. We then show in section 3 and section 4 the properties of weak and mean square convergence of the numerical solution towards the exact solution of the ODE. In section 5 we analyse the accuracy of Monte Carlo estimators drawn from the numerical solution. The geometric properties of the numerical scheme are presented in section 6 and section 7, while in section 8 we introduce Bayesian inverse problems in the ODE setting, and show how our method can be integrated in existing sampling strategies. Finally, we show a variety of numerical experiments confirming our theoretical results in section 9.

2. Random time step Runge-Kutta method.

Let us consider a Lipschitz function $f\colon \mathbb{R}^d \to \mathbb{R}^d$ and the ODE

$$y' = f(y), \quad y(0) = y_0 \in \mathbb{R}^d. \tag{2.1}$$

In the following, we will write for simplicity the solution $y(t)$ of (2.1) in terms of the flow of the ODE. In particular, we consider the family $\{\varphi_t\}_{t\geq 0}$ of functions $\varphi_t \colon \mathbb{R}^d \to \mathbb{R}^d$ such that

$$y(t) = \varphi_t(y_0). \tag{2.2}$$

Given a time step h, let us consider a Runge-Kutta method which approximates deterministically the solution $\varphi_t(y_0)$ of (2.1). In particular, we can write the numerical solution y_k approximating $\varphi_{t_k}(y_0)$, with $t_k = kh$ in terms of the numerical flow $\{\Psi_t\}_{t\geq 0}$, with $\Psi_t \colon \mathbb{R}^d \to \mathbb{R}^d$, which is uniquely determined by the coefficients of the method, as

$$y_{k+1} = \Psi_h(y_k), \quad k = 0, 1, \dots. \tag{2.3}$$

In order to provide a probabilistic interpretation of the numerical solution rather than a series of punctual values, Conrad et al. propose the scheme defined by

$$Y_{k+1} = \Psi_h(Y_k) + \xi_k(h), \quad k = 0, 1, \dots, \tag{2.4}$$

where Y_k is a random variable approximating $y(t_k)$ with $Y_0 = y_0$, and $\xi_k(h)$ are opportunely scaled independent and identically distributed (i.i.d.) random variables with values in $\mathbb{R}^d$. Maintaining the same notation as in (2.4), in this work we propose a random time-stepping Runge-Kutta method (RTS-RK), i.e., the scheme defined defined by the recurrence relation

$$Y_{k+1} = \Psi_{H_k}(Y_k), \quad k = 0, 1, \dots, \tag{2.5}$$

where Y_k is still a random variable approximating $y(t_k)$ and the time steps H_k are locally given by a sequence of i.i.d. random variables with values in $\mathbb{R}^+$. A graphical representation of one step of the RTS-RK method is given in Figure 3.

Remark 2.1. In terms of computational cost simulating the two methods (2.5) and (2.4) are almost equivalent, as they imply the same number of function evaluations as the underlying deterministic solver Ψ_h. Nonetheless, the random time-stepping method has the slight advantage that the random variable that has to be drawn at each time step takes values in $\mathbb{R}_+$, while for the additive noise ξ_k takes values in $\mathbb{R}^d$.

2.1. Assumptions and notations. We now present the main assumptions and notations which are used throughout the rest of this work. Firstly, we have to consider the possible values taken by the random step sizes, which have to satisfy restrictions that are necessary not to spoil the properties of deterministic methods.

Assumption 2.2. The i.i.d. random variables H_k satisfy for all $k = 0, 1, \dots$

(i) $H_k > 0$ a.s.,

(ii) there exists $h > 0$ such that $\mathbb{E}\, H_k = h$,

(iii) there exists $p \geq 1$ such that the scaled random variables $Z_k := H_k - h$ satisfy

$$\mathbb{E}\, Z_k^2 = Ch^{2p}, \tag{2.6}$$

which is equivalent to $\mathbb{E}\, H_k^2 = h^2 + Ch^{2p}$.

The class of random variable satisfying the hypotheses above is general. However, it is practical for an implementation point of view to have examples of these variables.

Example 2.3. Let us consider the random variables $\{H_k\}_{k\geq 0}$ such that

$$H_k \overset{\text{i.i.d.}}{\sim} \mathcal{U}(h-h^p, h+h^p), \quad 0<h<1, \quad p\geq 1. \tag{2.7}$$

We easily verify that the assumptions (i) and (ii) are verified as $h<1$, and that (iii) is verified with $C=1/3$. Another choice of random variables could simply be

$$H_k \overset{\text{i.i.d.}}{\sim} \log\mathcal{N}\big(\log h - \log\sqrt{1+h^{2p-2}}, \log(1+h^{2p-2})\big), \tag{2.8}$$

for which the properties above are trivially verified (with $C=1$), provided $p>1$.

We secondly introduce an assumption on the deterministic method underlying the RTS-RK scheme, identified by its numerical flow Ψ_h.

Assumption 2.4. The Runge-Kutta method defined by the numerical flow $\{\Psi_t\}_{t\geq 0}$ satisfies the following properties.

(i) For h small enough, there exists a constant $C>0$ such that

$$\|\Psi_h(y)-\varphi_h(y)\| \leq Ch^{q+1}, \quad \forall y\in\mathbb{R}^d, \tag{2.9}$$

i.e., the deterministic solver has order q.

(ii) The map $t\mapsto\Psi_t(y)$ is of class $C^2(\mathbb{R}^+,\mathbb{R}^d)$ and Lipschitz continuous of constant L_Ψ, i.e.,

$$\|\Psi_t(y)-\Psi_s(y)\| \leq L_\Psi|t-s|, \quad \forall t,s>0. \tag{2.10}$$

3. Weak convergence analysis. The first property of the RTS-RK method we wish to analyze is its weak convergence, which gives an indication about the behavior of the numerical solution (2.5) in the mean sense. Let us define the weak order of convergence.

Definition 3.1. *The numerical method* (2.5) *has weak order* r *for* (2.1) *if for any function* $\Phi\in\mathcal{C}^\infty(\mathbb{R}^d,\mathbb{R})$ *with all derivatives bounded uniformly on* $\mathbb{R}^d$ *there exists a constant* $C>0$ *independent of* h *such that*

$$|\mathbb{E}\,\Phi(Y_k)-\Phi(y(kh))| \leq Ch^r, \tag{3.1}$$

for all $k=1,2,\ldots,N$ *and* $T=Nh$.

Let us introduce the Lie derivative of the flow $\mathcal{L}=f\cdot\nabla$, which allows us to adopt the semi-group notation for the exact solution of (2.1) and write for any smooth function Φ

$$\Phi(\varphi_h(y)) = e^{h\mathcal{L}}\Phi(y). \tag{3.2}$$

Moreover, let us remark that the probabilistic numerical solution $\{Y_k\}_{k\geq 0}$ forms an homogeneous Markov chain, and hence there exists an operator $\mathcal{P}_t$, the infinitesimal generator, such that

$$\mathbb{E}\left(\Phi(Y_k)\mid Y_0=y\right) = (\mathcal{P}_{t_k}\Phi)(y). \tag{3.3}$$

The family of operators $\{\mathcal{P}_t\}_{t\geq 0}$ forms a Markov semi-group together with the associativity operation

$$(\mathcal{P}_{t+s}\Phi)(y) = \mathcal{P}_t(\mathcal{P}_s\Phi)(y). \tag{3.4}$$

In order to have an analogy with the notation (3.2), we adopt the exponential form of the infinitesimal generator and denote in the following $\mathcal{P}_t = e^{t\mathcal{L}^h}$, where we explicitely write the dependence of the Markov generator on the step size h. We can now state a result of local weak convergence of the probabilistic numerical solution.

Lemma 3.2 (Weak local order). *Let Assumption 2.2 and Assumption 2.4 hold. If* $\mathbb{E}\,|H_0^4| < \infty$, *there exists a constant* $C > 0$ *independent of* h *such that for any function* $\Phi \in \mathcal{C}^\infty(\mathbb{R}^d, \mathbb{R})$ *with all derivatives bounded uniformly on* $\mathbb{R}^d$

$$|\mathbb{E}(\Phi(Y_1) \mid Y_0 = y) - \Phi(\varphi_h(y))| \leq Ch^{\min\{2p,q+1\}}. \tag{3.5}$$

Proof. Let us expand the functional Φ computed on the numerical solution as

$$\begin{aligned}
\Phi(Y_1) &= \Phi(\Psi_{H_0}(Y_0)) \\
&= \Phi\Big(\Psi_h(Y_0) + (H_0 - h)\partial_t\Psi_h(Y_0) + \frac{1}{2}(H_0 - h)^2\partial_{tt}\Psi_h(Y_0) + \mathcal{O}(|H_0 - h|^3)\Big) \\
&= \Phi(\Psi_h(Y_0)) + \Big((H_0 - h)\partial_t\Psi_h(Y_0) + \frac{1}{2}(H_0 - h)^2\partial_{tt}\Psi_h(Y_0)\Big)\cdot\nabla\Phi(\Psi_h(Y_0)) \\
&\quad + \frac{1}{2}(H_0 - h)^2\partial_t\Psi_h(Y_0)\partial_t\Psi_h(Y_0)^\top : \nabla^2\Phi(\Psi_h(Y_0)) + \mathcal{O}(|H_0 - h|^3),
\end{aligned} \tag{3.6}$$

where we denote by $\nabla^2\Phi$ the Hessian matrix of Φ, and by : the inner product on matrices induced by the Frobenius norm on $\mathbb{R}^d$, i.e., $A : B = \mathrm{tr}(A^\top B)$. Taking the conditional expectation with respect to $Y_0 = y$ and applying Assumption 2.2 we get

$$\begin{aligned}
e^{h\mathcal{L}^h}\Phi(y) - \Phi(\Psi_h(y)) &= \frac{1}{2}Ch^{2p}\partial_{tt}\Psi_h(y)\cdot\nabla\Phi(\Psi_h(y)) \\
&\quad + \frac{1}{2}Ch^{2p}\partial_t\Psi_h(y)\partial_t\Psi_h(y)^\top : \nabla^2\Phi(\Psi_h(y)) + \mathcal{O}(h^{3p}),
\end{aligned} \tag{3.7}$$

where we exploited Hölder inequality for the last term. Moreover, expanding Φ in y we get

$$\begin{aligned}
\Phi(\Psi_h(y)) &= \Phi\left(\Psi_0(y) + h\partial_t\Psi_0(y) + \mathcal{O}(h^2)\right) \\
&= \Phi(y) + \mathcal{O}(h).
\end{aligned} \tag{3.8}$$

which implies

$$\begin{aligned}
e^{h\mathcal{L}^h}\Phi(y) - \Phi(\Psi_h(y)) &= \frac{1}{2}Ch^{2p}\partial_{tt}\Psi_h(y)\cdot\nabla\Phi(y) \\
&\quad + \frac{1}{2}Ch^{2p}\partial_t\Psi_h(y)\partial_t\Psi_h(y)^\top : \nabla^2\Phi(y) + \mathcal{O}(h^{2p+1}).
\end{aligned} \tag{3.9}$$

Let us remark that thanks to Assumption 2.4.(i) we have

$$e^{h\mathcal{L}}\Phi(y) - \Phi(\Psi_h(y)) = \mathcal{O}(h^{q+1}). \tag{3.10}$$

Combining (3.10) and (3.9) we have the one-step weak error of the probabilistic method on the original ODE, i.e.,

$$e^{h\mathcal{L}}\Phi(y) - e^{h\mathcal{L}^h}\Phi(y) = \mathcal{O}(h^{\min\{2p,q+1\}}), \tag{3.11}$$

which proves the desired result. ∎

In order to obtain a result on the global order of convergence we need a further stability assumption, which is the same as Assumption 3 in [6].

Assumption 3.3. The function f is such that the operator $e^{h\mathcal{L}^h}$ satisfies for all functions $\Phi \in \mathbb{C}^\infty(\mathbb{R}^d, \mathbb{R})$ with all derivatives uniformly bounded in $\mathbb{R}^d$ and a positive constant L

$$\sup_{u\in\mathbb{R}^d} |e^{h\mathcal{L}^h}\Phi(u)| \leq (1 + Lh) \sup_{u\in\mathbb{R}^d} |\Phi(u)|. \tag{3.12}$$

Remark 3.4. Given the assumptions on f and Φ above, it is true for the exact solution that

$$\sup_{u\in\mathbb{R}^d} |e^{h\mathcal{L}}\Phi(u)| \leq (1 + Lh) \sup_{u\in\mathbb{R}^d} |\Phi(u)|. \tag{3.13}$$

We can now state the main result on weak convergence. Let us remark that the theorem and its proof are similar to Theorem 2.4 in [6].

Theorem 3.5 (Weak order). *Let the assumptions of Lemma 3.2 and Assumption 3.3 hold. Then, there exists a constant $C > 0$ independent of h such that for all functions $\Phi \in \mathcal{C}^\infty(\mathbb{R}^d, \mathbb{R})$ with all derivatives bounded in $\mathbb{R}^d$*

$$|\mathbb{E}\,\Phi(Y_k) - \Phi(y(kh)))| \leq Ch^{\min\{2p-1,q\}}, \tag{3.14}$$

for all $k = 1, 2, \ldots, N$ and $T = Nh$.

Proof. Let us introduce the following notation

$$\begin{aligned} w_k(u) &= \Phi(\varphi_{t_k}(u)), \\ W_k(u) &= \mathbb{E}(\Phi(Y_k) \mid Y_0 = u). \end{aligned} \tag{3.15}$$

By the triangular inequality and the associativity property of $\exp(t\mathcal{L}^h)$, we have

$$\sup_{u\in\mathbb{R}^d} |W_k(u) - w_k(u)| \leq \sup_{u\in\mathbb{R}^d} |e^{h\mathcal{L}} w_{k-1}(u) - e^{h\mathcal{L}^h} w_{k-1}(u)| + \sup_{u\in\mathbb{R}^d} |e^{h\mathcal{L}^h} w_{k-1}(u) - e^{h\mathcal{L}^h} W_{k-1}(u)|. \tag{3.16}$$

We then apply Lemma 3.2 to the first term and Assumption 3.3 to the second, thus obtaining

$$\sup_{u\in\mathbb{R}^d} |W_k(u) - w_k(u)| \leq Ch^{\min\{2p,q+1\}} + (1 + Lh) \sup_{u\in\mathbb{R}^d} |w_{k-1}(u) - W_{k-1}(u)|. \tag{3.17}$$

Proceeding iteratively on the index k and noticing that $w_0 = W_0$, we obtain

$$\begin{aligned} \sup_{u\in\mathbb{R}^d} |w_k(u) - W_k(u)| &\leq Ckh^{\min\{2p,q+1\}} \\ &\leq CTh^{\min\{2p-1,q\}}, \end{aligned} \tag{3.18}$$

which proves the result for any chosen initial condition y_0 in $\mathbb{R}^d$, as

$$|\mathbb{E}\,\Phi(Y_k) - \Phi(y(kh)))| \le \sup_{u\in\mathbb{R}^d} |W_k(u) - w_k(u)|. \tag{3.19}$$

■

Remark 3.6. In [6], Conrad et al. define ordinary and stochastic modified equations in order to prove a result of weak convergence applying techniques of backward error analysis. In particular, they show that their probabilistic solver approximates in the weak sense a stochastic differential equation (SDE) where the deterministic part is given by the original ODE. For our probabilistic solver, it is possible to prove that the numerical solutions approximates in the weak sense the solution of an SDE where the diffusion term depends on the derivative of the map $t \mapsto \Psi_t(y)$.

4. Mean square convergence analysis. The second property of (2.5) we analyze is its mean square order of convergence, which gives an indication on the path-wise distance between each realisation of the numerical solution and the exact solution of (2.1). Let us define the mean square order of convergence.

Definition 4.1. *The numerical method* (2.5) *has mean square order of convergence* r *for* (2.1) *if there exists a constant* $C > 0$ *independent of* h *such that*

$$\left(\mathbb{E}\|Y_k - y(kh)\|^2\right)^{1/2} \le Ch^r \tag{4.1}$$

for all $k = 1, 2, \dots, N$ *and* $T = Nh$.

Remark 4.2. Let us remark that the mean square convergence is stronger than the traditional strong convergence, as for Jensen's inequality

$$\mathbb{E}\,\|Y_k - y(kh)\| \le \left(\mathbb{E}\|Y_k - y(kh)\|^2\right)^{1/2} \le Ch^r. \tag{4.2}$$

We start by analysing how the method converges with respect to the mean step size h in the local sense, i.e., after one step of the numerical integration.

Lemma 4.3 (Local mean square convergence). *Under Assumption* 2.2 *and Assumption* 2.4 *the numerical solution* Y_1 *given by one step of the RTS-RK method* (2.5) *satisfies*

$$\left(\mathbb{E}\|Y_1 - y(h)\|^2\right)^{1/2} \le Ch^{\min\{p,q+1\}}, \tag{4.3}$$

where C *is a real positive constant independent of* h *and the coefficients* p, q *are given in the assumptions.*

Proof. By triangular and Young's inequalities we have for all $y \in \mathbb{R}^d$

$$\mathbb{E}\|\Psi_{H_0}(y) - \varphi_h(y)\|^2 \le 2\,\mathbb{E}\|\Psi_{H_0}(y) - \Psi_h(y)\|^2 + 2\|\Psi_h(y) - \varphi_h(y)\|^2. \tag{4.4}$$

We now consider Assumption 2.4 and Assumption 2.2, thus getting

$$\begin{aligned} \mathbb{E}\|\Psi_{H_0}(y) - \varphi_h(y)\|^2 &\le 2L_\Psi^2\,\mathbb{E}|H_0 - h|^2 + 2C_1h^{2(q+1)} \\ &= 2L_\Psi^2 C_2 h^{2p} + 2C_1h^{2(q+1)} \\ &\le C^2h^{2\min\{q+1,p\}}, \end{aligned} \tag{4.5}$$

which is the desired result with $C = \max\{2L_\Psi^2C_2, 2C_1\}^{1/2}$. ■

As a consequence of the one-step convergence, we can prove a result of global mean square convergence.

Theorem 4.4 (Global mean square convergence). *Let f be globally Lipschitz and $t_k = kh$ for $k = 1, 2, \ldots, N$, where $Nh = T$. Then, under the assumptions of Lemma 4.3 the numerical solution given by (2.5) satisfies*

$$\sup_{k=1,2,\ldots,N} \left(\mathbb{E}\|Y_k - y(t_k)\|^2 \right)^{1/2} \leq Ch^{\min\{p-1/2,q\}}, \tag{4.6}$$

where C is a real positive constant independent of h.

In order to prove this result, let us introduce the following standard lemmas.

Lemma 4.5. *Given the ODE (2.1) with f globally Lipschitz, then for any y and w in $\mathbb{R}^d$ and $h < 1$ we have*

$$\|\varphi_h(y) - \varphi_h(w)\| \leq (1 + Ch)\|y - w\|, \tag{4.7}$$

$$\|\varphi_h(y) - \varphi_h(w) - (y - w)\| \leq Ch\|y - w\|, \tag{4.8}$$

where C is a positive constant independent of h.

Lemma 4.6. *Suppose that for arbitrary N and $k = 0, \ldots, N$ we have*

$$u_k \leq (1 + Ah)u_{k-1} + Bh^r, \tag{4.9}$$

where $h = T/N$, $A > 0$, $B \geq 0$, $r \geq 1$ and $u_k \geq 0, k = 0, \ldots, N$. Then

$$u_k \leq e^{AT}u_0 + \frac{B}{A}(e^{AT} - 1)h^{r-1}. \tag{4.10}$$

The proofs of these lemmas are standard and thus omitted in this work. We can now prove the main result on mean square convergence.

Proof of Theorem 4.4. In the following, we denote by C a generic positive constant. Let us define $e_k^2 := \mathbb{E}\|Y_k - y(t_k)\|^2$. Adding and subtracting the exact flow applied to the numerical solution, we obtain

$$\begin{aligned} e_{k+1}^2 = {} & \mathbb{E}\|\Psi_{H_k}(Y_k) - \varphi_h(Y_k)\|^2 + \mathbb{E}\|\varphi_h(Y_k) - \varphi_h(y(t_k))\|^2 \\ & + 2\,\mathbb{E}\left(\varphi_h(Y_k) - \varphi_h(y(t_k)), \Psi_{H_k}(Y_k) - \varphi_h(Y_k)\right), \end{aligned} \tag{4.11}$$

where we denote by $(\cdot, \cdot)$ the inner product in $\mathbb{R}^d$. Let us consider the three terms in (4.11) separately. For the first term, we have by Lemma 4.3

$$\mathbb{E}\|\Psi_{H_k}(Y_k) - \varphi_h(Y_k)\|^2 \leq Ch^{\min\{2p,2(q+1)\}}. \tag{4.12}$$

For the second term, since φ_h is Lipschitz with constant $(1 + Ch)$, we have

$$\mathbb{E}\|\varphi_h(Y_k) - \varphi_h(y(t_k))\|^2 \leq (1 + Ch)^2 e_k^2. \tag{4.13}$$

Let us now define $Z = \varphi_h(Y_k) - \varphi_h(y(t_k)) - (Y_k - y(t_k))$. Then we, can rewrite the inner product as

$$\begin{aligned}\mathbb{E}\left(\varphi_h(Y_k) - \varphi_h(y(t_k)), \Psi_{H_k}(Y_k) - \varphi_h(Y_k)\right) &= \mathbb{E}\left(Y_k - y(t_k), \Psi_{H_k}(Y_k) - \varphi_h(Y_k)\right) \\ &\quad + \mathbb{E}\left(Z, \Psi_{H_k}(Y_k) - \varphi_h(Y_k)\right).\end{aligned} \tag{4.14}$$

We bound the two terms in (4.14) separately. For the first term, by the law of total expectation, we have

$$\begin{aligned}\mathbb{E}\left(\left(Y_k - y(t_k)\right)^\top \left(\Psi_{H_k}(Y_k) - \varphi_h(Y_k)\right)\right) &= \mathbb{E}\,\mathbb{E}\left(\left(Y_k - y(t_k)\right)^\top \left(\Psi_{H_k}(Y_k) - \varphi_h(Y_k)\right) \mid Y_k\right) \\ &= \mathbb{E}\left(\left(Y_k - y(t_k)\right)^\top \mathbb{E}\left(\Psi_{H_k}(Y_k) - \varphi_h(Y_k) \mid Y_k\right)\right).\end{aligned} \tag{4.15}$$

Applying Cauchy-Schwarz inequality to the outer expectation we get

$$\begin{aligned}\mathbb{E}\left(\left(Y_k - y(t_k)\right)^\top \left(\Psi_{H_k}(Y_k) - \varphi_h(Y_k)\right)\right) &\le \left(\mathbb{E}\|\mathbb{E}\left(\Psi_{H_k}(Y_k) - \varphi_h(Y_k) \mid Y_k\right)\|^2\right)^{1/2} e_k \\ &\le C h^{\min\{2p, q+1\}} e_k,\end{aligned} \tag{4.16}$$

where we applied Lemma 3.2. We now consider the second term in (4.14). By Cauchy-Schwarz inequality we have

$$\mathbb{E}\left(Z, \Psi_{H_k}(Y_k) - \varphi_h(Y_k)\right) \le \left(\mathbb{E}\|Z\|^2\right)^{1/2} \left(\mathbb{E}\|\Psi_{H_k}(Y_k) - \varphi_h(Y_k)\|^2\right)^{1/2}. \tag{4.17}$$

We now apply Lemma 4.5 and Lemma 4.3 to obtain

$$\mathbb{E}\left(Z, \Psi_{H_k}(Y_k) - \varphi_h(Y_k)\right) \le C h^{\min\{p+1, q+2\}} e_k. \tag{4.18}$$

We can hence bound the scalar product in (4.14) with Young's inequality and assuming $h < 1$ as

$$\begin{aligned}\mathbb{E}\left(\varphi_h(Y_k) - \varphi_h(y(t_k)), \Psi_{H_k}(Y_k) - \varphi_h(Y_k)\right) &\le C(h^{\min\{p+1, q+2\}}) e_k \\ &\le \frac{h e_k^2}{2} + C\frac{h^{\min\{2p+1, 2q+1\}}}{2}.\end{aligned} \tag{4.19}$$

Combining (4.12), (4.13) and (4.19), we have

$$e_{k+1}^2 \le C h^{\min\{2p, 2q+1\}} + (1 + Ch) e_k^2, \tag{4.20}$$

which implies the desired result by Lemma 4.6 and since $e_0 = 0$. ∎

Remark 4.7. Let us remark that the difference between global and local orders of convergence is not exactly one, as it usually is in the purely deterministic case. In fact, thanks to the independence of the random variables there is only a $1/2$ loss in the random part of the exponent, while the natural loss of one order is verified in the deterministic component.

Remark 4.8. The result of mean square convergence suggests that a reasonable choice for the noise scale p is to fix it to $q + 1/2$, where q is the order of the Runge-Kutta method Ψ_h. In this way, the properties of convergence of the underlying deterministic method are not spoiled, nonetheless getting a probabilistic interpretation of the numerical solution.

5. Monte Carlo estimators. The third property we analyze is the mean-square convergence of Monte Carlo estimators drawn from the random time-stepping Runge-Kutta method. Let us consider a function $\Phi \in \mathcal{C}^\infty(\mathbb{R}^d, \mathbb{R})$ with Lipschitz constant L_Φ and a final time $T > 0$. Moreover, let us introduce the notation $Z = \Phi(y(T))$ and $Z_N = \Phi(Y_N)$. In general, the quantity Z_N is not accessible, and we have to replace it by its Monte Carlo estimator

$$\hat{Z}_N = M^{-1} \sum_{i=1}^{M} \Phi(Y_N^{(i)}), \tag{5.1}$$

where $T = hN$ is the final time, M is the number of trajectories and we denote by $\{Y_N^{(i)}\}_{i=1}^M$ a set of realizations of the numerical solution. Hence, we are interested in studying the mean square error of the Monte Carlo estimator, which is defined as

$$\mathrm{MSE}(\hat{Z}_N) = \mathbb{E}(Z - \hat{Z}_N)^2. \tag{5.2}$$

In the following result, we prove that this quantity converges to zero independently of the number of trajectories M.

Theorem 5.1. *Under Assumption 2.2 and Assumption 2.4, the Monte Carlo estimator $\hat{Z}$ satisfies*

$$\mathrm{MSE}(\hat{Z}_N) \leq C\left(h^{2\min\{2p-1,q\}} + \frac{h^{2\min\{p-1/2,q\}}}{M}\right), \tag{5.3}$$

where C is a positive constant independent of h and M.

Proof. Thanks to the classic decomposition of the MSE, we have

$$\mathrm{MSE}(\hat{Z}_N) = \mathrm{Var}\,\hat{Z} + \left(\mathbb{E}(\hat{Z} - Z)\right)^2. \tag{5.4}$$

Applying Theorem 3.5 to the second term, we have

$$\mathrm{MSE}(\hat{Z}_N) \leq \mathrm{Var}\,\hat{Z} + Ch^{2\min\{2p-1,q\}}. \tag{5.5}$$

The variance of the estimator can be trivially bounded exploiting the Lipschitz continuity of Φ and the independence of the samples by

$$\mathrm{Var}\,\hat{Z}_N \leq M^{-1} L_\Phi^2\, \mathbb{E}\|Y_N - y(T)\|^2. \tag{5.6}$$

Applying Theorem 4.4 we get

$$\mathrm{Var}\,\hat{Z}_N \leq M^{-1} L_\Phi^2 C h^{2\min\{q,p-1/2\}}, \tag{5.7}$$

which proves the desired result. ∎

Let us remark that with the choice $p = q + 1/2$, which is the minimum p for which the order of convergence of the underlying deterministic method is not affected by the probabilistic setting, we have $\mathrm{MSE}(\hat{Z}_N) \leq Ch^{2q}$ with $M = 1$. Hence, the Monte Carlo estimators drawn from (2.5) converge in the mean square sense independently of the number of samples M in (5.1). In the sub-optimal case $p < q + 1/2$, one should carefully select the number of trajectories M so that the two terms in (5.3) are balanced.

6. Conservation of first integrals. Numerical methods for ODEs are often studied in terms of their geometric properties [7]. In particular, we investigate here whether the random choice of time steps in (2.5) spoils the properties of the underlying deterministic Runge-Kutta method. Let us recall the definition of first integral for an ODE.

Definition 6.1. *Given a function $I\colon \mathbb{R}^d \to \mathbb{R}$, then $I(y)$ is a first integral of (2.1) if $I'(y)f(y) = 0$ for all $y \in \mathbb{R}^d$.*

If this property of the ODE is conserved by a numerical integrator, i.e., if for the any $y \in \mathbb{R}^d$ it is true that $I(\Psi_h(y)) = I(y)$, then we say that the numerical method conserves the first integral. In particular, this implies that the invariant is conserved along the trajectory of the numerical solution, i.e., $I(y_k) = I(y_0)$ for all $k \geq 0$.

Example 6.2. To illustrate this concept we first discuss the case of linear first integrals, which can be seen as a general case of the conservation of mass in physical systems. Let us consider a linear first integral $I(y) = v^\top y$ and any Runge-Kutta method with coefficients $\{b_i\}_{i=1}^s$, $\{a_{ij}\}_{i,j=1}^s$. Then, we have for a time step $H_0 > 0$

$$I(Y_1) = v^\top y_0 + H_0 \textstyle\sum_{i=1}^s b_i v^\top f(y_0 + H_0 \sum_{j=1}^s a_{ij} K_j), \tag{6.1}$$

where $\{K_i\}_{i=1}^s$ are the internal stages of the Runge-Kutta method. Since $I(y)$ is a first integral, $v^\top f(y) = 0$ for any $y \in \mathbb{R}^d$. Hence $I(Y_1) = I(y_0)$ and iteratively $I(Y_k) = I(y_0)$ for all $k \geq 0$ along the numerical trajectory. The equality above shows that any RTS-RK method conserves linear first integrals path-wise, or in the strong sense.

It is known that no Runge-Kutta method can conserve any polynomial invariant of order $n \geq 3$ [7]. Nonetheless, for some particular problems there exist tailored Runge-Kutta methods which can conserve polynomial invariants of higher order. We therefore can state the following general result.

Theorem 6.3. *If the Runge-Kutta scheme defined by Ψ_h conserves an invariant $I(y)$ for an ODE, then the numerical method (2.5) conserves $I(y)$ for the same ODE.*

Proof. If $I(\Psi_h(y)) = I(y)$ for any h, then $I(\Psi_{H_0}(y)) = I(y)$ for any value that H_0 can assume. ∎

We now consider quadratic first integrals, i.e., first integrals of the form $I(y) = y^\top C y$ with C a symmetric matrix, which are conserved by Runge-Kutta methods that satisfy the hypotheses of Cooper's theorem [7]. The conservation of quadratic first invariants is of the utmost importance, e.g., for Hamiltonian systems, as it implies the symplecticity of the scheme. It is known [7] that all Gauss methods conserve quadratic first integrals. The simplest member of this class of methods is the implicit midpoint rule, which is a one-stage method defined by coefficients $b_1 = 1$ and $a_{11} = 1/2$.

Corollary 6.4. *If the Runge-Kutta scheme defined by Ψ_h conserves quadratic first integrals then the numerical method (2.5) conserves quadratic first integrals.*

This result is a direct consequence of Theorem 6.3.

The properties above for the RTS-RK method are not satisfied by the additive noise method presented in [6]. In particular, let us remark that the conservation of first integrals

is exact for any trajectory of the RTS-RK method, and is not an average property. In other words, we can say that (2.5) conserves linear first integrals in the strong sense. For the additive noise numerical method (2.4), we have

$$\begin{aligned} I(Y_1) &= v^\top y_0 + h\textstyle\sum_{i=1}^s b_i v^\top f(y_0 + h\sum_{j=1}^s a_{ij}K_j) + v^\top \xi_0(h), \\ &= v^\top (y_0 + \xi_0(h)). \end{aligned} \tag{6.2}$$

If the random variable ξ_0 is zero-mean, then $\mathbb{E}\, I(Y_1) = I(y_0)$ and iteratively along the solution $\mathbb{E}\, I(Y_k) = I(y_0)$. Linear first integrals are therefore conserved in average, but not in a path-wise fashion.

For quadratic first integrals, we have instead that the additive noise method does not conserve them neither path-wise nor in the weak sense, as we have

$$\begin{aligned} I(Y_1) &= (\Psi_h(y_0) + \xi_0(h))^\top S(\Psi_h(y_0) + \xi_0(h)) \\ &= I(y_0) + 2\xi_0(h)^\top S\Psi_h(y_0) + \xi_0(h)^\top S\xi_0(h). \end{aligned} \tag{6.3}$$

If the random variables are zero-mean and if there exists a matrix Q such that $\mathbb{E}\, \xi_0(h)\xi_0(h)^\top = Qh^{2p+1}$ for some $p \geq 1$ (Assumption 1 in [6]) we then have

$$\mathbb{E}\, I(Y_1) = I(y_0) + Q : Sh^{2p+1}. \tag{6.4}$$

Hence, along the trajectories of the solution a bias is introduced in the first integral which persists even in the mean sense. In general, Theorem 6.3 is not valid for the additive noise method, as the random contribution drives the first integral far from its true value at each time step. This could produce in practice large deviations of the numerical approximation from the true solution, especially in the long time regime.

7. Hamiltonian systems. A class of dynamical systems of particular interest for their geometric properties are the Hamiltonian systems. Given a function $Q\colon \mathbb{R}^{2d} \to \mathbb{R}$, called the Hamiltonian, they can be written as

$$y' = J^{-1}\nabla Q(y), \quad y(0) = y_0 \in \mathbb{R}^{2d}, \tag{7.1}$$

where the matrix $J \in \mathbb{R}^{2d\times 2d}$ is defined as

$$J = \begin{pmatrix} 0 & I \\ -I & 0 \end{pmatrix}, \tag{7.2}$$

and where I is the identity matrix in $\mathbb{R}^{d\times d}$. The Hamiltonian Q is a first integral for (7.1), hence we require numerical integrators to conserve the energy, or at least not to deviate from its true value in an uncontrolled fashion. As it was shown in the previous section, when Q is a polynomial it is possible to obtain exact conservation with deterministic integrators and with their probabilistic counterparts obtained with the RTS-RK method. If Q is not a polynomial, exact conservation is in general not achievable, but a good approximation of the energy over long time spans is achievable through the notion of symplectic differentiable maps.

Definition 7.1 (Definition VI.2.2 in [7]). *A differentiable map $g\colon U \to \mathbb{R}^{2d}$ (where $U \subset \mathbb{R}^{2d}$ is an open set) is called symplectic if the Jacobian matrix g' is everywhere symplectic, i.e., if*

$$(g')^\top J g' = J. \tag{7.3}$$

It is well-known that the flow $\varphi_t\colon \mathbb{R}^{2d} \to \mathbb{R}^{2d}$ of any system of the form (7.1) is symplectic. In a natural manner, a numerical integrator is called symplectic if its numerical flow Ψ_h is a symplectic map. In the following, we will analyse both the local and global properties of the RTS-RK method built on symplectic integrators and applied to (7.1).

7.1. Local symplecticity of the RTS-RK method. It has been pointed out [16, 7] that applying an adaptive step size technique to a symplectic method can destroy its symplecticity. Therefore, Skeel and Gear [16] write any adaptive technique in function of a map $\tau(y,h)$ such that the k-th time step h_k is selected as $h_k = \tau(y_k, h)$, where h is a base value for the time step. Hence, in order to have again a symplectic method, the new condition to be satisfied is

$$V^\top J V = J, \quad V = \partial_y \Psi_{\tau(y,h)}(y) + \partial_t \Psi_{\tau(y,h)}(y) \partial_y \tau(y,h)^\top. \tag{7.4}$$

Let us now consider the RTS-RK method based on a symplectic deterministic integrator. We have the following lemma.

Lemma 7.2. *If the flow Ψ_h of the deterministic integrator is symplectic, then the flow of the random time-stepping probabilistic method (2.5) is symplectic.*

Proof. For the RTS-RK scheme, the k-th time step H_k is selected via a random mapping $\tau(y,h) = \tau(h) = h\Theta_k$, where Θ_k are opportunely scaled random variables such that H_k satisfies Assumption 2.2. Hence, τ is independent of y and with the notation introduced above

$$V = \partial_y \Psi_{\tau(h)}(y). \tag{7.5}$$

Therefore, by the symplecticity of Ψ_t the condition $V^\top J V = J$ is satisfied and the flow map of the RTS-RK method is symplectic. ∎

Let us remark that the local symplecticity of the flow map does not imply alone a good conservation of the Hamiltonian for the numerical solution. Global properties of approximation of the energy are therefore presented below.

7.2. Global strong conservation of the Hamiltonian. We now wish to study the mean conservation of the Hamiltonian along the trajectories of the RTS-RK method based on symplectic integrators. Our goal is obtaining a bound on the quantity $\mathbb{E}|Q(Y_n) - Q(y_0)|$, possibly valid for large values of the time index n. As stated above, showing theoretically long time conservation of the energy function in Hamiltonian systems requires backward error analysis. In the following, we will introduce the bases of this technique and show how they apply to our probabilistic integrator.

The first ingredient needed to perform a rigorous backward error analysis is a rather strong assumption on the regularity of the ODE.

Assumption 7.3 (see e.g. [7], Section IX.7). The function f is analytic in a neighbourhood of the initial condition y_0 and there exist constants $M, R > 0$ such that $\|f(y)\| \leq M$ for $\|y - y_0\| \leq 2R$.

In general, backward error analysis is based on determining a modified equation $y' = \tilde{f}(y)$ such that the numerical approximation is its exact solution. Hence, the function $\tilde{f}$ will both depend on the original ODE and on the numerical flow map Ψ_h. In particular, for an integrator of order q the modified equation is given by a function $\tilde{f}$ defined as

$$\tilde{f}(y) = f(y) + h^q f_{q+1}(y) + h^{q+1} f_{q+2}(y) + \dots, \tag{7.6}$$

where the functions $\{f_i\}_{i>q}$ are uniquely determined by f, its derivatives and by the coefficients of the Runge-Kutta method. The exactness of the numerical solution for the modified equation is nonetheless only formal, as the infinite sum defining $\tilde{f}$ is not guaranteed to converge. Thus, it is necessary to truncate the sum in order to perform a rigorous analysis, i.e.,

$$\tilde{f}(y) = f(y) + h^q f_{q+1}(y) + h^{q+1} f_{q+2}(y) + \dots + h^{N-1} f_N(y). \tag{7.7}$$

where $q < N < \infty$ is the truncation index. Let us remark that in the following we will always refer to the truncated function above when using the symbol $\tilde{f}$. Moreover, we denote by $\tilde{\varphi}_{N,t}$ the exact flow of the equation $y' = \tilde{f}(y)$. The property of exactness of the numerical solution for the modified equation is trivially lost by a truncation of the infinite sum, and the numerical error committed over one step of integration is given by the following Lemma.

Lemma 7.4 (see e.g. [7], Section IX.7). *Under assumption 7.3 and for h sufficiently small, there exists $N = N(h)$ such that the numerical flow Ψ_h and the exact flow of the truncated modified equation $\tilde{\varphi}_{N,h}$ satisfy*

$$\|\Psi_h(y_0) - \tilde{\varphi}_{N,h}(y_0)\| \leq Che^{-\kappa/h}, \tag{7.8}$$

where C and κ are positive constants depending only on the method's coefficients and on the regularity of the function f.

It is possible to prove that for an Hamiltonian system (7.1) and a symplectic integrator the modified equation is still an Hamiltonian system, i.e., there exists a modified Hamiltonian $\tilde{Q}$ defined as

$$\tilde{Q}(y) = Q(y) + h^q Q_{q+1}(y) + \dots + h^{N-1} Q_N(y). \tag{7.9}$$

such that $\tilde{f} = J^{-1}\nabla\tilde{Q}$. Hence, the modified Hamiltonian is conserved along the trajectories of the modified equation, which together with Lemma 7.4 guarantees a good approximation of the original Hamiltonian over long time spans, as stated in the following Theorem.

Theorem 7.5 (see e.g. [7], Section IX.8). *Under assumption 7.3 and for h sufficiently small, if the numerical solution y_n given by a symplectic method of order q applied to an Hamiltonian system is close enough to the initial condition y_0, then for exponentially long times*

$$\tilde{Q}(y_n) = \tilde{Q}(y_0) + \mathcal{O}(e^{-\kappa/2h}), \tag{7.10}$$

$$Q(y_n) = Q(y_0) + \mathcal{O}(h^q). \tag{7.11}$$

The results presented above summarise the properties of conservation of the energy function for deterministic symplectic integrators. The randomisation in the time step implies that a general modified equation does not exist. Nonetheless, thanks to the assumptions on the time steps, it is possible to prove that the Hamiltonian is still well approximated in the strong sense, as shown by the following result.

Theorem 7.6. *Under Assumption 7.3 and Assumption 2.2 and if the numerical solution Y_n is close enough to the initial condition y_0 almost surely, there exist constants $C_1, C_2 > 0$ independent of h such that the solution given by the RTS-RK method built on a symplectic integrator applied to a Hamiltonian system with Hamiltonian Q satisfies*

$$\mathbb{E}|Q(Y_n) - Q(y_0)| \leq C_1 h^q + C_2 \sqrt{t} h^{p+q-1/2}. \tag{7.12}$$

Proof. We exploit the conservation of $\tilde{Q}$ along the trajectories of the modified Hamiltonian system, i.e., $\tilde{Q}(\tilde{\varphi}_{N,z}(y)) = \tilde{Q}(y)$ for $y \in \mathbb{R}^d$ and $z > 0$ and employ a telescopic sum to obtain

$$\begin{aligned} \mathbb{E}\left(\tilde{Q}(Y_n) - \tilde{Q}(y_0)\right) &= \sum_{j=1}^{n} \mathbb{E}\left(\tilde{Q}(Y_j) - \tilde{Q}(Y_{j-1})\right) \\ &= \sum_{j=1}^{n} \mathbb{E}\left(\tilde{Q}(Y_j) - \tilde{Q}(\tilde{\varphi}_{N,h}(Y_{j-1}))\right). \end{aligned} \tag{7.13}$$

We then add and subtract the modified Hamiltonian computed on the numerical flow with fixed time step h to obtain

(7.14)

$$\begin{aligned} \mathbb{E}|\tilde{Q}(Y_n) - \tilde{Q}(y_0)| &\leq \sum_{j=0}^{n-1} \mathbb{E}|\tilde{Q}(Y_{j+1}) - \tilde{Q}(\Psi_h(Y_j)) + \tilde{Q}(\Psi_h(Y_j)) - \tilde{Q}(\tilde{\varphi}_{N,h}(Y_j))| \\ &\leq \sum_{j=0}^{n-1} \mathbb{E}|\tilde{Q}(\Psi_{H_j}(Y_j)) - \tilde{Q}(\Psi_h(Y_j))| + \sum_{j=0}^{n-1} \mathbb{E}|\tilde{Q}(\Psi_h(Y_j)) - \tilde{Q}(\tilde{\varphi}_{N,h}(Y_j))| \\ &= \sum_{j=0}^{n-1} \mathbb{E}|I_{1,j}| + \sum_{j=0}^{n-1} \mathbb{E}|I_{2,j}|, \end{aligned}$$

where $I_{1,j} = \tilde{Q}(\Psi_{H_j}(Y_j)) - \tilde{Q}(\Psi_h(Y_j))$ and $I_{2,j} = \tilde{Q}(\Psi_h(Y_j)) - \tilde{Q}(\tilde{\varphi}_{N,h}(Y_j))$. Let us first consider the second term. Thanks to Lemma 7.4 and since $\tilde{Q}$ is Lipschitz-continuous, we have

$$\sum_{j=0}^{n-1} \mathbb{E}|I_{2,j}| \leq nCe^{-\kappa/h}. \tag{7.15}$$

Hence, this term is bounded by $e^{-\kappa/2h}$ for exponentially long time spans, i.e., for $n \leq e^{\kappa/2h}$. For the first term, we consider the Taylor expansion of the numerical solution, which can be written for any $y \in \mathbb{R}^{2d}$ and $h > 0$ as

$$\Psi_h(y) = y + hJ^{-1}\nabla Q(y) + h^2 d_2(y) + \dots \tag{7.16}$$

where the d_i functions are analytic and bounded thanks to Assumption 7.3 (see [7, Theorem IX.7.2]). Moreover, thanks to Assumption 7.3 we can compute a Taylor expansion of $\tilde{Q}$ and obtain for each $j = 0, \dots, n-1$

$$I_{1,j} = \nabla\tilde{Q}(Y_j)^\top J^{-1}\nabla Q(Y_j)(H_j - h) + \mathcal{O}((H_j^2 - h^2)). \tag{7.17}$$

Let us denote by $S\colon \mathbb{R}^{2d} \to \mathbb{R}$ the function $S(y) = Q_{q+1}(y) + hQ_{q+2}(y) + \ldots + h^{N-1-q}Q_N(y)$, i.e., $\tilde{Q}(y) = Q(y) + h^q S(y)$, and remark that

$$\begin{aligned}\nabla\tilde{Q}(Y_j)^\top J^{-1}\nabla Q(Y_j) &= \nabla Q(Y_j)^\top J^{-1}\nabla Q(Y_j) + h^q\nabla S(Y_j)^\top J^{-1}\nabla Q(Y_j)\\ &= h^q\nabla S(Y_j)^\top J^{-1}\nabla Q(Y_j),\end{aligned} \tag{7.18}$$

since Q is a first integral of motion for (7.1). Thanks to Assumption 2.2 and Assumption 7.3, we can write $I_{1,j} = h^q\eta_j$ for a sequence of independent random variables $\{\eta_j\}_{j=0}^{n-1}$ such that $\mathbb{E}\,\eta_j = 0$ and $\operatorname{Var}\eta_j \le Ch^{2p}$ for a constant $C > 0$ independent of h. Hence, by Jensen's inequality we get

$$\begin{aligned}\sum_{j=0}^{n-1}\mathbb{E}|I_{1,j}| &\le h^q\Big(\mathbb{E}\,(\sum_{j=0}^{n-1}|\eta_j|)^2\Big)^{1/2} = h^q\Big(\sum_{j=0}^{n-1}\mathbb{E}\,\eta_j^2\Big)^{1/2}\\ &\le Cn^{1/2}h^{p+q} = Ct^{1/2}h^{p+q-1/2}.\end{aligned} \tag{7.19}$$

Considering Assumption 7.3 and applying the triangular inequality we have

$$\begin{aligned}\mathbb{E}|Q(Y_n) - Q(y_0)| &\le h^q\big(\mathbb{E}|S(Y_n)| + |S(y_0)|\big) + \mathbb{E}|\tilde{Q}(Y_n) - \tilde{Q}(y_0)|\\ &\le C_1h^q + C_2t^{1/2}h^{p+q-1/2},\end{aligned} \tag{7.20}$$

which is the desired result. ∎

Remark 7.7. The result of Theorem 7.6 is consistent with the theory of deterministic symplectic integrators. In fact, in the deterministic limit $p \to \infty$, we have

$$\mathbb{E}|Q(Y_n) - Q(y_0)| = \mathcal{O}(h^q), \tag{7.21}$$

and the expectation $\mathbb{E}\,Q(Y_n) \to Q(y_n)$, where y_n is the numerical solution given by the deterministic method. Moreover, choosing the natural scale for the noise $p = q + 1/2$, we have

$$\mathbb{E}|Q(Y_n) - Q(y_0)| \le C_3h^q + C_4t^{1/2}h^{2q}, \tag{7.22}$$

which guarantees that $\mathbb{E}|Q(Y_n) - Q(y_0)| = \mathcal{O}(h^q)$ for time intervals of length $t = \mathcal{O}(h^{-2q})$. Let us remark that this is the same accuracy that would be obtained employing a deterministic symplectic method. Nonetheless, the RTS-RK approximation is valid over polynomial time spans instead of exponential time spans as in the deterministic case.

8. Bayesian inference inverse problems. It has been recently shown [6, 4] that probabilistic methods for ordinary and partial differential equations guarantee good results in the context of Bayesian inverse problems. In this section, we briefly introduce a Bayesian inverse problem in the ODE setting and how the RTS-RK method can be employed in this framework.

Let us consider a function $f_\vartheta\colon \mathbb{R}^d \to \mathbb{R}^d$ which depends on a real parameter $\vartheta \in \Theta$ where Θ is an open subset of $\mathbb{R}^n$ and the ODE

$$y'_\vartheta = f_\vartheta(y), \quad y_\vartheta(0) = y_0 \in \mathbb{R}^d. \tag{8.1}$$

In order to simplify the notation, we consider y_0 to be a fixed initial condition. In general, y_0 could depend itself on ϑ. In the classical setting of numerical analysis, the main problem of interest is to determine the solution y_ϑ given the parameter ϑ. The inverse problem we consider is instead to determine ϑ through observations of the solution y_ϑ or of quantities derived from it. In the Bayesian setting, the inverse problem is recast in terms of probability distributions, and the goal is to establish a probability measure on ϑ, the posterior measure, given observations and all the prior knowledge available.

Let us denote by $\mathcal{Y} \in \mathbb{R}^m$ the observable and by $\mathcal{G}\colon \Theta \to \mathbb{R}^m$ the forward operator, which can be written as $\mathcal{G} = \mathcal{O} \circ \mathcal{S}$, where $\mathcal{S}$ is the solution operator and $\mathcal{O}$ is the observation operator. In this case, $\mathcal{S}\colon \mathbb{R}^n \to \mathcal{C}([0,T])$ is the operator mapping ϑ into the solution y_ϑ, and $\mathcal{O}\colon \mathcal{C}([0,T]) \to \mathbb{R}^m$ maps the solution into the observable. Observations are then given by evaluations of the forward model corrupted by noise. In particular, we model noise as a Gaussian random variable $\varepsilon \sim \mathcal{N}(0, \Sigma_\varepsilon)$ independent of ϑ, so that observations read

$$\mathcal{Y} = \mathcal{G}(\vartheta) + \varepsilon. \tag{8.2}$$

Under these assumptions, the likelihood of the observations can be written as

$$\pi(\mathcal{Y} \mid \vartheta) = e^{-V_\mathcal{Y}(\vartheta)}, \tag{8.3}$$

where the function $V_\mathcal{Y}\colon \Theta \to \mathbb{R}$, called potential or negative log-likelihood, is given by

$$V_\mathcal{Y}(\vartheta) = \frac{1}{2}\big(\mathcal{G}(\vartheta) - \mathcal{Y}\big)^\top \Sigma_\varepsilon^{-1}\big(\mathcal{G}(\vartheta) - \mathcal{Y}\big). \tag{8.4}$$

The second building block of Bayesian inverse problems is the prior distribution, which we denote by $\pi_0(\vartheta)$. The prior encodes all the knowledge on the parameter that is known before observations are provided. In the following, we adopt a common abuse of notation, confounding measures and their probability density function.

Once the likelihood model and the prior distribution are established, it is possible to compute the posterior distribution $\pi(\vartheta \mid \mathcal{Y})$ via Bayes' theorem, i.e.,

$$\pi(\vartheta \mid \mathcal{Y}) = \frac{\pi(\mathcal{Y} \mid \vartheta)\pi_0(\vartheta)}{Z(\mathcal{Y})}, \tag{8.5}$$

where $Z(\mathcal{Y})$ is the normalising constant given by

$$Z(\mathcal{Y}) = \int_\Theta \pi(\mathcal{Y} \mid \vartheta)\pi_0(\vartheta)\,\mathrm{d}\vartheta. \tag{8.6}$$

Let us denote by $\mathcal{G}^h(\vartheta)$ the forward model where the solution operator is approximated by a Runge-Kutta method with time step h, and consequently with $V_{\mathcal{Y}}^h(\vartheta)$ and $\pi^h(\mathcal{Y} \mid \vartheta)$ the potential and the likelihood function obtained replacing $\mathcal{G}(\vartheta)$ with $\mathcal{G}^h(\vartheta)$. We can then define analogously the approximated posterior distribution $\pi^h(\vartheta \mid \mathcal{Y})$ via Bayes' formula. In [17, Theorem 4.6], Stuart proves that the posterior distribution $\pi^h(\vartheta \mid \mathcal{Y})$ converges to $\pi(\vartheta \mid \mathcal{Y})$ with respect to h with the same rate as $V_{\mathcal{Y}}^h(\vartheta)$ converges to $V_{\mathcal{Y}}(\vartheta)$. Convergences is proved in the Hellinger distance, which is defined for probability density functions as

$$d_{\text{Hell}}\big(\pi^h(\vartheta \mid \mathcal{Y}), \pi(\vartheta \mid \mathcal{Y})\big)^2 = \frac{1}{2}\int_\Theta \Big(\sqrt{\pi^h(\vartheta \mid \mathcal{Y})} - \sqrt{\pi(\vartheta \mid \mathcal{Y})}\Big)^2 \,\mathrm{d}\vartheta. \tag{8.7}$$

Hence, when there is no restriction in computational resources and it is possible to choose h small, the approximated posterior distribution can be pushed arbitrarily close to the true posterior.

In this work we consider the case when h is fixed, and in particular we are interested in the case where the numerical error dominates the noise contribution. It has been shown empirically [6, 5] that in this small noise limit the approximated posterior distributions can be overly confident on the value of the parameter. In particular, the expectation of ϑ computed under the posterior distribution presents a bias with respect to the true value, which is not highlighted by higher order moments. This undesirable phenomenon can be corrected employing a probabilistic method, as the one presented by Conrad et al. in [6] or the RTS-RK method, to approximate the potential $V_{\mathcal{Y}}(\vartheta)$. Let us denote by $\xi \in \mathcal{X}$ the auxiliary random variable introduced by the probabilistic method. In the case of RTS-RK, we have $\xi = (H_0, H_1, \dots, H_{N-1})^\top$ and $\mathcal{X} \subset \mathbb{R}_+^N$. The likelihood function, denoted as $\pi_{\text{pr}}^h(\mathcal{Y} \mid \vartheta)$ is then approximated as

$$\pi_{\text{pr}}^h(\mathcal{Y} \mid \vartheta) = \mathbb{E}^\xi\, e^{-V_{\mathcal{Y}}^{h,\xi}(\vartheta)}. \tag{8.8}$$

where $V_{\mathcal{Y}}^{h,\xi}$ is the approximation of the potential function given by the probabilistic method. The corresponding posterior distribution π_{pr}^h is then obtained as

$$\pi_{\text{pr}}^h(\vartheta \mid \mathcal{Y}) = \frac{\pi_{\text{pr}}^h(\mathcal{Y} \mid \vartheta)\pi_0(\vartheta)}{\mathbb{E}^\xi\, Z^{h,\xi}(\mathcal{Y})}, \tag{8.9}$$

where the normalising constant is given by

$$Z^{h,\xi}(\mathcal{Y}) = \int_\Theta e_{\mathcal{Y}}^{-V^{h,\xi}}(\vartheta)\pi_0(\vartheta)\mathrm{d}\vartheta. \tag{8.10}$$

Modifying the posterior in this manner allows to obtain qualitatively better results, which account for the uncertainty introduced by the numerical solver. Moreover, this posterior distribution still converges to the true posterior for $h \to 0$ as proved in [13], where (8.9) is called the marginal posterior.

In order to sample from the posteriors defined above we employ Markov chain Monte Carlo (MCMC) algorithms. In particular, thanks to the way the probabilistic posterior (8.9) is defined, the pseudo-marginal Metropolis Hastings (PMMH) algorithm [3] is a suitable choice for sampling. In case of a deterministic approximation of the forward model, we employ the standard random walk Metropolis Hastings.

8.1. Analytical posteriors in a linear problem. In the limited case of linear problems and Gaussian prior it is possible to write explicitly the posterior distributions. Let us hence consider the following one dimensional ODE

$$y'(t) = -y(t), \quad y(0) = y_0. \tag{8.11}$$

Given $h > 0$, we consider the inferential problem of determining the true initial condition y_0^* from a single observation $d = \varphi_h(y_0^*) + \varepsilon$, where $\varphi_h(y_0^*) = y_0^* e^{-h}$ is the true solution at time $t = h$ and $\varepsilon \sim \mathcal{N}(0, \sigma^2)$ is a source of noise. If a Gaussian prior $\pi_0 = \mathcal{N}(0, 1)$ is given for y_0, the true posterior distribution is computable analytically and is given by

$$\pi(y_0 \mid d) = \mathcal{N}\Big(y_0; \frac{de^{-h}}{\sigma^2 + e^{-2h}}, \frac{\sigma^2}{\sigma^2 + e^{-2h}}\Big), \tag{8.12}$$

where $\mathcal{N}(x; \mu, \alpha^2)$ is the density of a Gaussian random variable of mean μ and variance α^2 evaluated in x. Consistently, if $\sigma^2 \to 0$, we have that $d \to y_0^* e^{-h}$ and therefore $\pi(y_0 \mid d) \to \delta_{y_0^*}$.

If we approximate $\varphi_h(y_0)$ for a given initial condition y_0 with a single step of the explicit Euler method (i.e., with step size h), we get $\Psi_h(y_0) = (1 - h)y_0$. Computing the posterior distribution obtained with this approximation leads to

$$\pi^h(y_0 \mid d) = \mathcal{N}\Big(y_0; \frac{(1-h)d}{\sigma^2 + (1-h)^2}, \frac{\sigma^2}{\sigma^2 + (1-h)^2}\Big). \tag{8.13}$$

In the limit of $\sigma^2 \to 0$, we get in this case that the posterior distribution tends to $\pi^h(y_0 \mid d) \to \delta_{\bar{y}}$, where $\bar{y} = e^{-h} y_0^*/(1 - h)$. The posterior distribution is hence tending to a biased Dirac delta with respect to the true value.

Let us consider the additive noise method (2.4) applied to the explicit Euler method, i.e., the random approximation $y(h) \approx Y_1$, where $Y_1 = (1 - h)y_0 + \xi$ and where $\xi \sim \mathcal{N}(0, h^3)$, so that the method converges consistently with the deterministic method. In this case, the posterior distribution that we denote by $\pi^h_{\mathrm{pr,AN}}$ is given by

$$\pi^h_{\mathrm{pr,AN}}(y_0 \mid d) = \mathcal{N}\Big(y_0; \frac{(1-h)d}{\tilde{\sigma}^2 + (1-h)^2}, \frac{\tilde{\sigma}^2}{\tilde{\sigma}^2 + (1-h)^2}\Big). \tag{8.14}$$

where $\tilde{\sigma}^2 = \sigma^2 + h^3$. Hence, taking the limit $\sigma^2 \to 0$ gives

$$\pi^h_{\mathrm{pr,AN}}(y_0 \mid d) \to \mathcal{N}\Big(y_0; \frac{(1-h)e^{-h}y_0^*}{h^3 + (1-h)^2}, \frac{h^3}{h^3 + (1-h)^2}\Big), \tag{8.15}$$

which shows that while the asymptotic mean is still biased with respect to the true value, the uncertainty in the forward model is reflected by a positive variance. Let us now consider the random time step explicit Euler with step size distribution $H \sim \mathcal{U}(h - h^p, h + h^p)$. In this case, the forward model acts as

$$Y_1 = y_0 - Hy_0 = (1 - h)y_0 + Uy_0, \quad U \sim \mathcal{U}(-h^p, h^p). \tag{8.16}$$

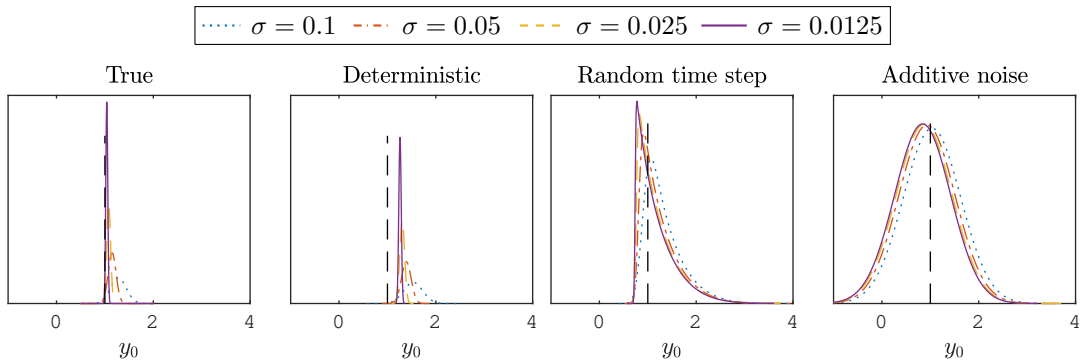

Figure 4: Analytical posterior distributions in the linear case of subsection 8.1 for the true solution and its approximations with the deterministic explicit Euler method and the two probabilistic versions with additive noise (2.4) and with random time steps (2.5). In this case, $h = 0.5$ and the variance σ^2 of the observation error is reduced progressively. The true value of the initial condition $y_0^* = 1$ is shown with a vertical black dashed line.

Hence, disregarding all multiplicative constants that are independent of y_0 and setting $p = q + 1/2 = 3/2$, we get the posterior

(8.17)
$$\pi^h_{\mathrm{pr,RTS}}(y_0 \mid d) \propto \exp\Big(-\frac{y_0^2}{2}\Big)\frac{1}{y_0}\Big(\Phi\Big(\frac{((1-h)+h^{3/2})y_0 - d}{\sigma}\Big) - \Phi\Big(\frac{((1-h)-h^{3/2})y_0 - d}{\sigma}\Big)\Big),$$

where Φ denotes the cumulative distribution function of a standard Gaussian random variable. In this case, the closed-form expression of the posterior distribution cannot be a Gaussian as the random variable H has to satisfy Assumption 2.2.(i). In the limit for $\sigma \to 0$, we get the limiting distribution

$$\pi^h_{\mathrm{pr,RTS}}(y_0 \mid d) \propto \exp\Big(-\frac{y_0^2}{2}\Big)\frac{1}{y_0}\chi_{\{y_{\min} \le y_0 \le y_{\max}\}}, \tag{8.18}$$

where $y_{\min}$ and $y_{\max}$ are given by

$$y_{\min} = \frac{e^{-h}y_0^*}{((1-h)+h^{3/2})}, \quad y_{\max} = \frac{e^{-h}y_0^*}{((1-h)-h^{3/2})}. \tag{8.19}$$

It is hence possible to remark that for the RTS-RK method the variance of the posterior distribution is not collapsing to zero for $\sigma \to 0$ as in the deterministic case.

We fix $h = 0.5$ and consider $\sigma = \{0.1, 0.05, 0.025, 0.0125\}$, thus generating four observational noises η_i as $\eta_i = \sigma_i Z$ for a random variable $Z \sim \mathcal{N}(0,1)$. In Figure 4 we show the posteriors (8.12), (8.13), (8.15) and (8.17), which confirm our claim, i.e., that probabilistic methods take into account the variability in the forward model caused by the numerical approximation and transfer it to the posterior belief.

9. Numerical experiments. In this section, we present a series of numerical experiments that illustrate the versatility and usefulness of our new random time stepping method. These experiments also corroborate the theoretical results presented in the previous sections.

Method	ET					RK4				
q			2					4		
p	1	1.5	2	2.5	3	3	3.5	4	4.5	5
$\min\{q, p-1/2\}$	0.5	1	1.5	2	2	2.5	3	3.5	4	4
strong order	0.51	1.02	1.54	2.01	2.01	2.50	3.01	3.56	4.02	4.01

Table 1: Mean square order of convergence for the random time-stepping explicit trapezoidal (ET) and fourth-order Runge-Kutta (RK4) as a function of the value of p of Assumption 2.2.

Method	ET			RK4				
q		2				4		
p	1	1.5	2	1	1.5	2	3	4
$\min\{q, 2p-1\}$	1	2	2	1	2	3	4	4
weak order	0.98	2.06	2.12	0.90	1.96	3.01	3.97	4.08

Table 2: Weak order of convergence for the random time-stepping explicit trapezoidal (ET) and fourth-order Runge-Kutta (RK4) as a function of the value of p of Assumption 2.2.

9.1. Mean square order of convergence. In order to verify the result predicted in Theorem 4.4, we consider the FitzHug-Nagumo equation, which is defined as

$$\begin{aligned} y_1' &= c\big(y_1 - \frac{y_1^3}{3} + y_2\big), \qquad y_1(0) = -1, \\ y_2' &= -\frac{1}{c}(y_1 - a + b y_2), \quad y_2(0) = 1, \end{aligned} \tag{9.1}$$

where a, b, c are real parameters with values $a = 0.2$, $b = 0.2$, $c = 3$. We integrate the equation from time $t_0 = 0$ to final time $T = 1$. The reference solution is generated with an high order method on a fine time scale. We consider as deterministic solvers the explicit trapezoidal rule and the classic fourth order Runge-Kutta method, which verify Assumption 2.4 with $q = 2$ and $q = 4$ respectively. Moreover, we consider random time steps as in Example 2.3, where we vary p in order to verify the order of convergence predicted in Theorem 4.4. We vary the mean time step h taken by the random time steps H_n in the range $h_i = 0.01 \cdot 2^{-i}$, with $i = 0, 1, \dots, 4$. Then, we simulate 10^3 realizations of the numerical solution Y_{N_i}, with $N_i = T/h_i$ for $i = 0, 1, \dots, 4$, and compute the approximate mean square order of convergence for each value of h with a Monte Carlo mean. Results (Table 1) show that the orders predicted theoretically by Proposition 4.4 are confirmed numerically.

9.2. Weak order of convergence. We now verify the weak order of convergence predicted in Theorem 3.5. For this experiment we consider the ODE (9.1) as well, with the same time scale and parameters as above. The reference solution at final time is generated in this case as well with an high-order method on a fine time scale. The deterministic integrators we choose in this experiment are the explicit trapezoidal rule and the classic fourth-order Runge-Kutta method. The mean time step varies in the range $h_i = 0.1 \cdot 2^{-i}$ with $i = 0, 1, \dots, 5$, and we vary the value of p in Assumption 2.2 in order to verify the theoretical result of Theorem 3.5.

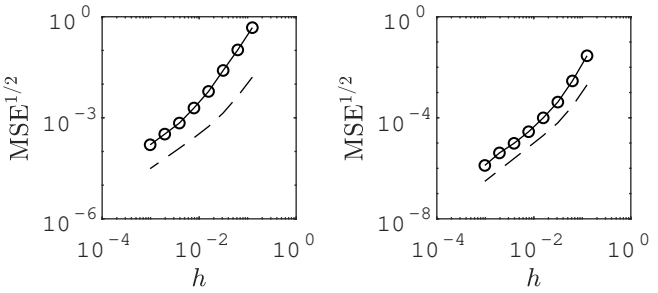

Figure 5: Convergence of the MSE of the Monte Carlo estimator for the random time-stepping explicit trapezoidal (ET) (left figure) and fourth-order Runge-Kutta (RK4) (right figure). The dashed line corresponds to the order predicted in Theorem 5.1 with $M = 10^3$ for ET and $M = 10^4$ for RK4.

The function $\Phi\colon \mathbb{R}^d \to \mathbb{R}$ of the solution we consider is defined as $\varphi(x) = x^\top x$. Finally, we consider 10^6 trajectories of the numerical solution in order to approximate the expectation with a Monte Carlo sum. Results (Table 2) show that the order of convergence predicted theoretically is confirmed by numerical experiments.

9.3. Monte Carlo estimator. We shall now verify numerically the validity of Theorem 5.1. We consider the ODE (9.1), with final time $T = 1$ and the same parameters as above. In this case as well, we consider the explicit trapezoidal rule and the fourth-order explicit Runge-Kutta method with random time steps having mean $h_i = 0.125 \cdot 2^{-i}$ with $i = 0, 1, \dots, 7$. For the explicit trapezoidal rule, we fix $M = 10^3$ and $p = 1.5$, so that for bigger values of h the first term in the bound presented in Theorem 5.1 dominates, while in the regime of small h, the higher order of the first term makes the second term larger in magnitude. This behaviour results in the change of slope in the convergence plot which can be observed in Figure 5, both in the theoretical estimate and in the numerical results. We perform the same experiment using the fourth-order explicit Runge-Kutta method, fixing $M = 10^4$ and $p = 2$, thus obtaining a numerical confirmation of the theoretical result.

9.4. Robustness. In this numerical experiment we verify the robustness of RTS-RK when applied to chemical reactions. Let us consider the Peroxide-Oxide chemical reaction, which is macroscopically defined by the following balance equation

$$\mathrm{O_2} + 2\mathrm{NADH} + 2\mathrm{H^+} \to 2\mathrm{H_2O} + 2\mathrm{NAD^+}. \tag{9.2}$$

This reaction has to be catalyzed by an enzyme to take place, which reacts with the reagents to create intermediate products of the reaction. A successful model [15] to describe the time-evolution of the chemical system is the following

$$\begin{gathered} \mathrm{B} + \mathrm{X} \xrightarrow{k_1} 2\mathrm{X}, \quad 2\mathrm{X} \xrightarrow{k_2} 2\mathrm{Y}, \quad \mathrm{A} + \mathrm{B} + \mathrm{Y} \xrightarrow{k_3} 3\mathrm{X}, \\ \mathrm{X} \xrightarrow{k_4} \mathrm{P}, \quad \mathrm{Y} \xrightarrow{k_5} \mathrm{Q}, \quad \mathrm{X_0} \xrightarrow{k_6} \mathrm{X}, \\ \mathrm{A_0} \xleftrightarrow{k_7} \mathrm{A}, \quad \mathrm{B_0} \xrightarrow{k_8} \mathrm{B}. \end{gathered} \tag{9.3}$$

Here, A and B are respectively $[O_2]$ and [NADH], P, Q are the products and X, Y are intermediates results of the reaction process. It is therefore possible to model the time evolution of the reaction with the following system of nonlinear ODEs

$$\begin{aligned} \mathrm{A}' &= k_7(\mathrm{A}_0 - \mathrm{A}) - k_3\mathrm{ABY}, & \mathrm{A}(0) &= 6, \\ \mathrm{B}' &= k_8\mathrm{B}_0 - k_1\mathrm{BX} - k_3\mathrm{ABY}, & \mathrm{B}(0) &= 58, \\ \mathrm{X}' &= k_1\mathrm{BX} - 2k_2\mathrm{X}^2 + 3k_3\mathrm{ABY} - k_4\mathrm{X} + k_6\mathrm{X}_0, & \mathrm{X}(0) &= 0, \\ \mathrm{Y}' &= 2k_2\mathrm{X}^2 - k_5\mathrm{Y} - k_3\mathrm{ABY}, & Y(0) &= 0, \end{aligned} \tag{9.4}$$

where $\mathrm{A}_0 = 8$, $\mathrm{B}_0 = 1$, $\mathrm{X}_0 = 1$ and the real parameters k_i, $i = 1, \dots, 8$ representing the reaction rates take values

$$\begin{aligned} k_1 &= 0.35, \quad k_2 = 250, \quad k_3 = 0.035, \quad k_4 = 20, \\ k_5 &= 5.35, \quad k_6 = 10^{-5}, \quad k_7 = 0.1, \quad k_8 = 0.825. \end{aligned} \tag{9.5}$$

It has been shown [15] that for these values of the parameters the system exhibits a chaotic behavior. In particular, at long time the trajectories are captured in a strange attractor, and the system shows a strong sensitivity to perturbations on the initial condition.

Since the components of the solution represent the concentration of chemicals, we require the numerical solution to be positive. Apart from physical considerations, numerically we observe that if one of the components takes negative values, the solution shows strong instabilities. For the RTS-RK method, if the distribution of the random time steps is carefully selected, as for example in Example 2.3, the probability of obtaining a negative solution can be set to zero. In contrast, for the additive noise method we can have disruptive effects even for h small if the solution has a small magnitude, as the probability of turning negative cannot be set to zero. Hence, in this case employing the additive noise method likely produces instabilities regardless of the chosen time step.

Let us apply the additive noise method (2.4) and the random time-stepping scheme (2.5) to equation (9.4). We choose $h = 0.05$ as the mean time steps for (2.5) and as the time step for (2.4), while we employ the Runge-Kutta-Chebyshev method (RKC) [18] as deterministic integrator. The RKC method is a stabilized numerical integrator of first order, which allows to obtain stable solutions with an explicit scheme. Higher order explicit stabilized methods such as ROCK2 or ROCK4 [2, 1] could also be used as deterministic solvers for the RTS-RK method. It can be seen in Figure 6 that the RTS-RK method conserves the positivity of the numerical solution while capturing the chaotic nature of the chemical reaction, while the additive noise scheme produces negative values, thus showing strong instabilities in the long-time behavior.

9.5. Conservation of quadratic first integrals. A simple model for the two-body problem in celestial mechanics is the Kepler system with a perturbation, , which reads

$$\begin{aligned} q_1' &= p_1, \quad p_1' = -\frac{q_1}{\|q\|^3} - \frac{\delta q_1}{\|q\|^5}, \\ q_2' &= p_2, \quad p_2' = -\frac{q_2}{\|q\|^3} - \frac{\delta q_2}{\|q\|^5}, \end{aligned} \tag{9.6}$$

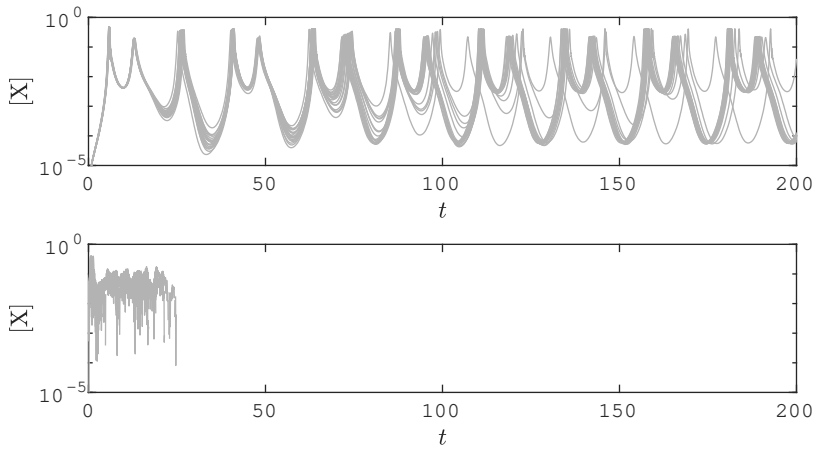

Figure 6: Fifty trajectories of the numerical value of the concentration of the X species for the random time-stepping and additive noise methods (above and below respectively).

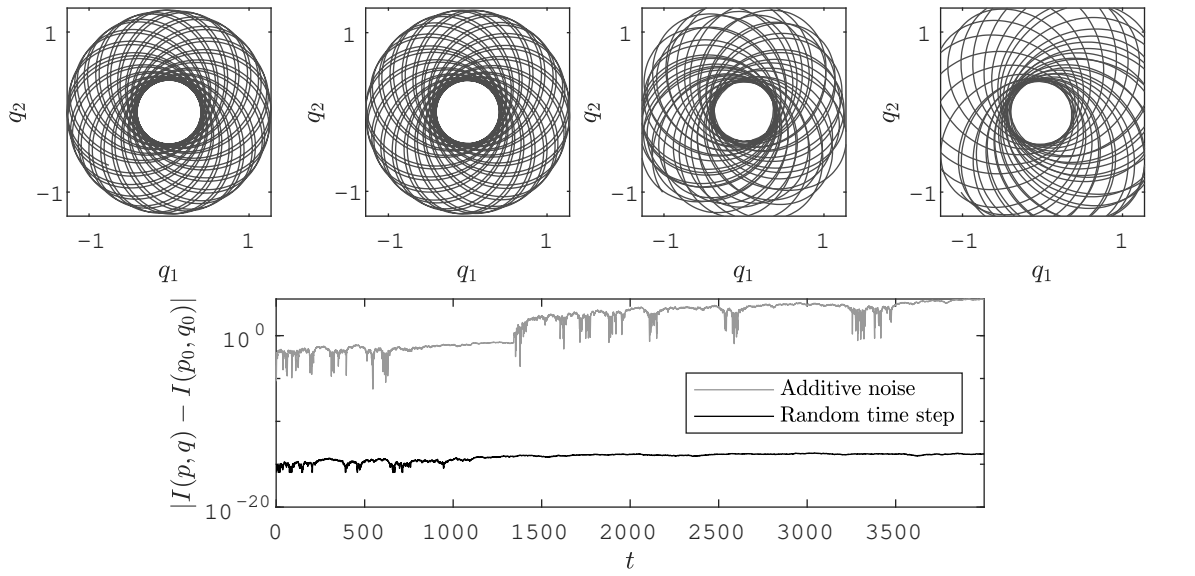

Figure 7: Trajectories of (9.6) given by the RTS-RK method (2.5) for $0 \leq t \leq 200$ and $3800 \leq t \leq 4000$ (first and second figures), and by the additive noise method (2.4) for $0 \leq t \leq 200$ and $200 \leq t \leq 400$ (third and fourth figures). Error on the angular momentum for $0 \leq t \leq 4000$ given by the two methods.

where p_1, p_2 are the two components of the velocity and q_1, q_2 are the two components of the position. We assume the perturbation parameter δ to be equal to 0.015 and the initial condition to be

$$q_1(0) = 1 - e, \quad q_2(0) = 0, \quad p_1(0) = 0, \quad p_2(0) = \sqrt{(1+e)/(1-e)}, \tag{9.7}$$

where $e = 0.6$ is the eccentricity. It is well-known that this equation has the Hamiltonian and the angular momentum as quadratic first integrals. In particular, we focus here on the

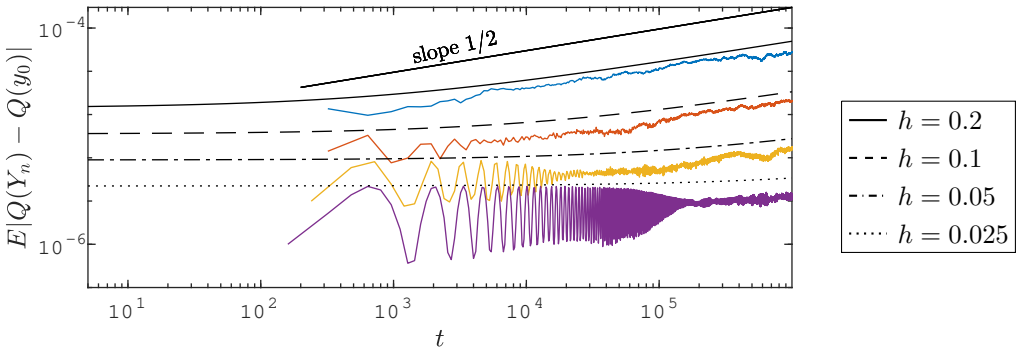

Figure 8: Time evolution of the mean error for the pendulum problem and different values of the time step h. The black lines represent the theoretical estimate given by the left hand side of equation (7.22), while the colored lines represent the experimental results. The mean was computed averaging 20 realisations of the numerical solution.

angular momentum, which reads

$$I(p,q) = q_1 p_2 - q_2 p_1. \tag{9.8}$$

We consider the simplest Gauss collocation method, namely the implicit midpoint rule, as the deterministic Runge-Kutta method. It is known that Gauss collocation methods conserve quadratic first integrals. According to Theorem 6.3, we expect therefore that the random time-stepping method (2.5) implemented with Ψ_h given by the implicit midpoint rule conserves also quadratic first integrals. We therefore integrate (9.6) with mean time step $h = 0.01$ from time $t = 0$ to time $t = 4000$ which corresponds to approximately 636 revolutions of the system (long-time behavior). Moreover, we consider the additive noise method (2.4) with $h = 0.01$, expecting that the first integral will not be conserved. We observe in Figure 7 that the method (2.5) conserves the angular momentum, while for the method (2.4) the approximate conservation of the quadratic first integral shown in (6.4) is lost when integrating (9.6) over long time.

9.6. Hamiltonian systems. Let us consider the pendulum problem, which is given by the Hamiltonian $Q\colon \mathbb{R}^2 \to \mathbb{R}$ defined by

$$Q(v,w) = \frac{v^2}{2} - \cos w, \tag{9.9}$$

where $y = (v,w)^\top \in \mathbb{R}^2$. We wish to study the validity of Theorem 7.6, i.e., show that the mean error on the Hamiltonian is of order $\mathcal{O}(h^q)$ for time spans of polynomial length and then it grows proportionally to the square root of time. We consider the initial condition $(v_0, w_0) = (1.5, -\pi)$ and integrate the equation employing RTS-RK based on the implicit midpoint method ($q = 2$) and choosing $p = q + 1/2 = 2.5$, which is the optimal scaling of the noise. We vary the mean time step $h \in \{0.2, 0.1, 0.05, 0.025\}$, integrate the dynamical system up to the final time $T = 10^6$ and study the time evolution of the mean numerical error on the Hamiltonian Q. Results are shown in Figure 8, where it is possible to notice that the error

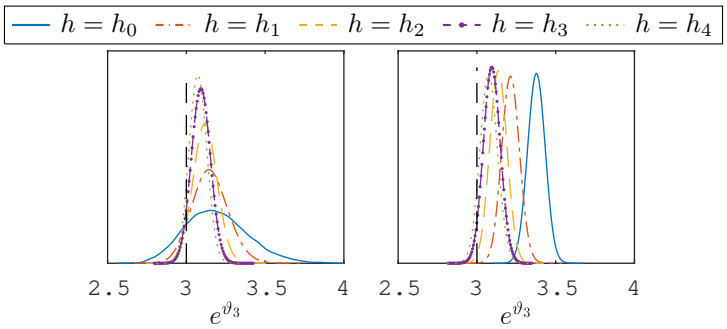

Figure 9: Posterior distribution for $\exp(\vartheta_3)$ obtained with the standard random walk Metropolis and the explicit Euler method (left picture) and the pseudo-marginal Metropolis-Hastings and RTS-RK explicit Euler method (right picture). In the plot, $h_i = 0.1 \cdot 2^{-i}$. The dashed vertical line indicates the true value of the parameter $\exp(\vartheta_3^*)$.

is growing with a rate $1/2$ in time after a stationary phase, where the term in h^q in (7.22) is dominating the term in $t^{1/2}h^{2q}$ due to the lower power of h. The oscillations of the error which are shown in Figure 8 are due to the term of order h^q and are present even when integrating the pendulum system with a deterministic symplectic scheme.

9.7. Bayesian inferential problems. For the last numerical experiment we revisit the FitzHug-Nagumo equation,

$$\begin{aligned} y'_{\vartheta,1} &= c\big(y_{\vartheta,1} - \frac{y_{\vartheta,1}^3}{3} + y_{\vartheta,2}\big), \quad y_{\vartheta,1}(0) = -1, \\ y'_{\vartheta,2} &= -\frac{1}{c}(y_{\vartheta,1} - a + b y_{\vartheta,2}), \quad y_{\vartheta,2}(0) = 1, \end{aligned} \tag{9.10}$$

where in the spirit of Bayesian inverse problems we consider $a, b, c \in \mathbb{R}$ to be unknown parameters. We recall that their true value is given by $a = 0.2$, $b = 0.2$ and $c = 3$, see equation (9.1). The test is then to infer the value of the parameter $\vartheta = (\vartheta_1, \vartheta_2, \vartheta_3)^\top = (\log a, \log b, \log c)^\top \in \mathbb{R}^3$ from observations of the solution of (9.10). The exponential transformation operated on each component of the parameter is taken to ensure positiveness of $(a, b, c)^\top$ for any value of ϑ. We consider the forward problem operator $\mathcal{G}\colon \mathbb{R}^n \to \mathbb{R}^m$ introduced in section 8 to be defined by

$$\mathcal{G}(\vartheta) = (y_\vartheta(0.1)^\top, y_\vartheta(0.2)^\top, \dots, y_\vartheta(1)^\top)^\top, \tag{9.11}$$

thus $n = 3$ and $m = 20$. Synthetic observations are then generated fixing ϑ to its true value $\vartheta^* = (\log(0.2), \log(0.2), \log(3))^\top$ and integrating the equation with a Runge-Kutta solver with a small time step and biased by Gaussian observational noise, i.e.,

$$\mathcal{Y} = \mathcal{G}(\vartheta) + \eta, \quad \eta \sim \mathcal{N}\big(0, (0.05)^2 I_{20}\big), \tag{9.12}$$

where I_r is the r-dimensional identity matrix. We fix the prior distribution on ϑ to be a standard Gaussian $\mathcal{N}(0, I_3)$. Let us remark that since the amount of noise in the observational model is small, this choice of prior does not yield information on the true value of the

parameter. We then sample from the posterior distributions $\pi^h(\vartheta \mid \mathcal{Y})$ and $\pi^h_{\rm pr}(\vartheta \mid \mathcal{Y})$ defined in section 8 and given by the explicit Euler method and its RTS-RK version employing the MH and the PMMH algorithms respectively. In both cases, we perform the MCMC algorithm for the step sizes $h_i = 0.1 \cdot 2^{-i}$, $i = 0, 1, 2, 3, 4$. In Figure 9 we show the marginal posterior for the parameter $\exp(\vartheta_3)$. We observe that for the coarser values of h the posterior $\pi^h(\vartheta \mid \mathcal{Y})$ is centred in a biased value in an overconfident manner, whereas for the same values of h, the posterior $\pi^h_{\rm pr}(\vartheta \mid \mathcal{Y})$ accounts better for the statistical uncertainty introduced by the discretisation error.

REFERENCES

[1] A. Abdulle, *Fourth order Chebyshev methods with recurrence relation*, SIAM J. Sci. Comput., 23 (2002), pp. 2041–2054.

[2] A. Abdulle and A. A. Medovikov, *Second order Chebyshev methods based on orthogonal polynomials*, Numer. Math., 90 (2001), pp. 1–18.

[3] C. Andrieu and G. O. Roberts, *The pseudo-marginal approach for efficient Monte Carlo computations*, Ann. Statist., 37 (2009), pp. 697–725.

[4] O. A. Chkrebtii, D. A. Campbell, B. Calderhead, and M. A. Girolami, *Bayesian solution uncertainty quantification for differential equations*, Bayesian Anal., 11 (2016), pp. 1239–1267.

[5] J. Cockayne, C. Oates, T. Sullivan, and M. Girolami, *Probabilistic numerical methods for PDE-constrained Bayesian inverse problems*, AIP Conference Proceedings, 1853 (2017), p. 060001.

[6] P. R. Conrad, M. Girolami, S. Särkkä, A. Stuart, and K. Zygalakis, *Statistical analysis of differential equations: introducing probability measures on numerical solutions*, Stat. Comput., (2016).

[7] E. Hairer, C. Lubich, and G. Wanner, *Geometric Numerical Integration. Structure-Preserving Algorithms for Ordinary Differential Equations*, Springer Series in Computational Mathematics 31, Springer-Verlag, Berlin, second ed., 2006.

[8] E. Hairer, S. P. Nørsett, and G. Wanner, *Solving Ordinary Differential Equations I. Nonstiff Problems*, vol. 8, Springer Verlag Series in Comput. Math., Berlin, 1993.

[9] E. Hairer and G. Wanner, *Solving ordinary differential equations II. Stiff and differential-algebraic problems*, Springer-Verlag, Berlin and Heidelberg, 1996.

[10] D. J. Higham and A. M. Stuart, *Analysis of the dynamics of local error control via a piecewise continuous residual*, BIT, 38 (1998), pp. 44–57.

[11] H. Kersting and P. Hennig, *Active uncertainty calibration in Bayesian ODE solvers*, in Proceedings of the 32nd Conference on Uncertainty in Artificial Intelligence (UAI 2016), AUAI Press, 2016, pp. 309–318.

[12] H. Lamba and A. M. Stuart, *Convergence results for the MATLAB* ODE23 *routine*, BIT, 38 (1998), pp. 751–780.

[13] H. C. Lie, T. Sullivan, and A. Teckentrup, *Random forward models and log-likelihoods in bayesian inverse problems*, arXiv preprint arXiv:1712.05717, (2017).

[14] E. N. Lorenz, *Deterministic nonperiodic flow*, J. Atmos. Sci., 20 (1963), pp. 130–141.

[15] L. F. Olsen, *An enzyme reaction with a strange attractor*, Phys. Lett. A, 94 (1983), pp. 454 – 457.

[16] R. D. Skeel and C. W. Gear, *Does variable step size ruin a symplectic integrator?*, Physica, 60 (1992), pp. 311–313.

[17] A. M. Stuart, *Inverse problems: A Bayesian perspective*, Acta Numer., 19 (2010), pp. 451–559.

[18] P. van der Houwen and B. P. Sommeijer, *On the internal stage Runge-Kutta methods for large m-values*, Z. Angew. Math. Mech., 60 (1980), pp. 479–485.